

A Fast Spectral Algorithm for Nonlinear Wave Equations with Linear Dispersion

Bengt Fornberg¹ and Tobin A. Driscoll²

Department of Applied Mathematics, CB-526, University of Colorado, Boulder, Colorado 80309

E-mail: fornberg@colorado.edu; tad@colorado.edu

Received April 21, 1999; revised August 10, 1999

Spectral algorithms offer very high spatial resolution for a wide range of nonlinear wave equations on periodic domains, including well-known cases such as the Korteweg–de Vries and nonlinear Schrödinger equations. For the best computational efficiency, one needs also to use high-order methods in time while somehow bypassing the usual severe stability restrictions. We use linearly implicit multistep methods, with the innovation of choosing different methods for different ranges in Fourier space—high accuracy at low wavenumbers and A -stability at high wavenumbers. This new approach compares favorably to alternatives such as split-step and integrating factor (or linearly exact) methods. © 1999 Academic Press

Key Words: spectral methods; nonlinear waves; KdV; NLS; linearly implicit.

1. INTRODUCTION

We consider the numerical solution of nonlinear wave equations of the form

$$u_t = N(u) + L(u) + g(x, t). \quad (1)$$

We restrict the description to one space dimension for notational simplicity, and we require the x -domain to be periodic. The function $N(u)$ is nonlinear and may depend also on u_x , etc.; we can embed the forcing function $g(x, t)$ into $N(u)$ and need not consider it further. The linear part is $L(u) = c(t)i^{m+1}(\partial^m u / \partial x^m)$, but more general linear dispersive terms are also treatable. The real function $c(t)$ is often a constant.

Many interesting equations are of the form (1), such as the Korteweg–de Vries equation,

$$u_t + 6uu_x + u_{xxx} = 0 \quad (\text{KdV})$$

¹ Supported by NSF DMS-9706919 and AFOSR/DARPA F49620-96-1-0426.

² Supported by an NSF Postdoctoral Research Fellowship and by an NSF Vigre Postdoctoral Fellowship under Grant DMS-9810751.

and the nonlinear Schrödinger equation,

$$iu_t + |u|^2u + u_{xx} = 0. \tag{NLS}$$

For these two examples, inverse scattering theory [15–17] provides analytic solutions in principle. These two equations often arise as leading-order approximations to nonlinear phenomena. In the few cases where analytical techniques remain available for more accurate models, their complexity is often prohibitive. Numerical techniques are usually more widely applicable. The algorithm presented here is designed to provide highly accurate solutions to all equations of the form (1) at the lowest possible computational cost.

The topics of the remaining sections are as follows:

2. Linearly implicit multistep methods for ordinary differential equations (ODEs)
3. The key idea behind the present algorithm
4. Stability analysis and refinement of ideas
5. Numerical comparisons to leading alternative methods
6. Conclusions

2. LINEARLY IMPLICIT MULTISTEP METHODS FOR ODES

Linear multistep methods [11] for solving the ODE $y' = f(t, y)$ use values of f at s consecutive time levels, requiring only one evaluation of f per time step. One way to view (and generate) the explicit Adams–Bashforth (AB) and implicit Adams–Moulton (AM) schemes is

$$y_{n+1} - y_n = \int_{t_n}^{t_{n+1}} \left(\text{interpolating poly-} \begin{cases} \text{AB: } t_{n-s}, t_{n-s+1}, \dots, t_n \\ \text{nominal for } f \text{ over } \left\{ \text{AM: } t_{n-s}, t_{n-s+1}, \dots, t_n, t_{n+1} \right\} \end{cases} \right) dt. \tag{2}$$

Following the notation in [6], we illustrate the stencils of linear multistep methods as shown in Fig. 1. Implicitness typically increases the stable time step size for a stiff problem but incurs the considerable cost of solving a (usually) nonlinear system at each time step.

Writing (1) in Fourier space as

$$\hat{u}_t = \hat{N}(\hat{u}) + \hat{L}(\hat{u}), \tag{3}$$

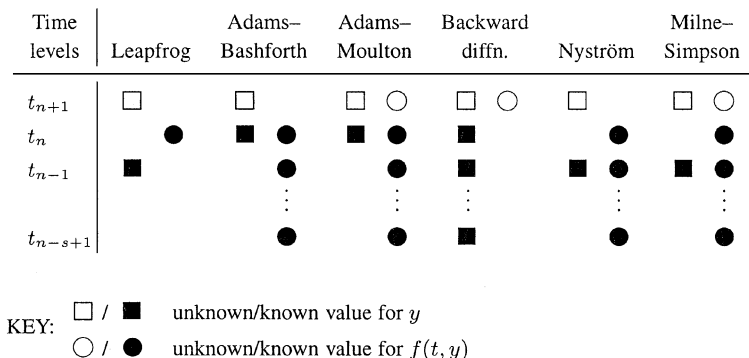


FIG. 1. Stencil notation for common multistep methods.

we can approximate it as

$$\hat{u}_{n+1} - \hat{u}_n = \int_{t_n}^{t_{n+1}} (\text{AB-type approx. for } \hat{N}(\hat{u})) dt + \int_{t_n}^{t_{n+1}} (\text{AM-type approx. for } \hat{L}(\hat{u})) dt. \quad (4)$$

In the case of, say, NLS, $\hat{N}(\hat{u})$ would be evaluated in physical space, and $\hat{L}(\hat{u}) = -i\omega^2\hat{u}$, where ω is the Fourier wavenumber. Using third-order Adams formulas, for example, we would obtain

$$\hat{u}_{n+1} = \left(1 - \frac{5}{12}k\hat{L}\right)^{-1} \left[\hat{u}_n + \frac{k}{12}(8\hat{L}(\hat{u}_n) - \hat{L}(\hat{u}_{n-1}) + 23\hat{N}(\hat{u}_n) - 16\hat{N}(\hat{u}_{n-1}) + 5\hat{N}(\hat{u}_{n-2})) \right].$$

(We present this for illustration only, not as a recommendation.) Since the \hat{L} -operator is diagonal, the need to invert the \hat{L} term does not incur any extra computational cost. This idea has appeared many times in the literature for both multistep and Runge–Kutta methods, often for diffusive problems and bearing a name such as “implicit–explicit” or “linearly implicit” [1–5].

Graphically, we illustrate a scheme of the form (4) in Fig. 2. Employing a slightly different \hat{u} -stencil than the one for AB/AM, this type of argument led Chan and Kerkhoven [5] to propose



for the KdV equation. Their method, which is applicable to any equation of the form (1), combines a standard leap-frog approximation for the nonlinear part with an A -stable trapezoidal (or Crank–Nicolson) rule for the linear part. Although a mild stability restriction is theoretically in force, conditions are far more favorable than the $k = O(h^3)$ and $k = O(h^2)$, respectively, that would normally be expected of approximations to (KdV) and (NLS); here h and k denote space and time steps, respectively. In practice this method is limited by second-order accuracy, not by stability.

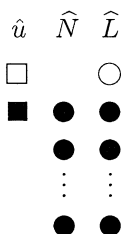


FIG. 2. Illustration of a linearly implicit AB/AM scheme. (It is not necessary in general that the \hat{N} and \hat{L} stencils stop at the same time level.)

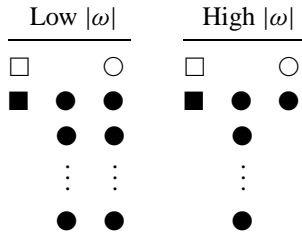
3. KEY IDEA BEHIND THE PRESENT ALGORITHM

To achieve high computational efficiency, we now consider higher-order methods of the form indicated by Fig. 2. Because we assume pure propagation problems, the linearization of the problem is expected to have purely imaginary spectrum. Hence we are primarily interested in the stability ordinate (extent of stability domain along the imaginary axis) of the constituent multistep methods. The stability ordinate is nonzero in the AB case only for orders 3,4, 7,8, 11,12, . . . and in the AM case only for orders 1,2, 5,6, 9,10, . . . (see [9, 10] and the proofs in [8]); hence, we must choose from among these methods.

Because no multistep method of order greater than 2 can be *A*-stable [12], we are seemingly faced with an unacceptable time step restriction from the linear $\hat{L}(\hat{u}) = i\omega^m \hat{u}$ term. However, we make some observations concerning the Fourier wavenumber ω :

1. For low values of $|\omega|$ (where most of a smooth solution’s “energy” is located), the time steps are accuracy- and not stability-limited, and
2. The ODEs for different ω can be treated with different multistep solvers. (Runge–Kutta methods, whose internal stages require identical information across all modes, do not allow the needed flexibility.)

A simple idea would therefore be: Given a time step k , use a higher-order scheme for as high $|\omega|$ as its stability ordinate allows, and elsewhere fall back to the *A*-stable AM2 for the linear part (henceforth we append an integer to indicate order of accuracy). This idea can be illustrated:



Terms such as “low” and “high” will be made precise later. This basic idea must be applied with some care. In the next section we show the necessity of two refinements:

1. The AM2 stencil is modified for the high- $|\omega|$ range, and
2. The low- $|\omega|$ range is further divided into a pure AB method and a linearly implicit AB/AM method.

4. STABILITY ANALYSIS

To study the stability of a linearly implicit multistep method, we linearize

$$\hat{u}_t = \hat{N}(\hat{u}) + \hat{L}(\hat{u})$$

to obtain

$$\hat{u}_t + i\alpha\hat{u} + i\beta\hat{u} = 0, \tag{5}$$

for real constants α and β . Clearly $\beta = \omega^m$, but the interpretation of α is less certain. We do assume that α is nonzero but of a lower order in ω than is β .

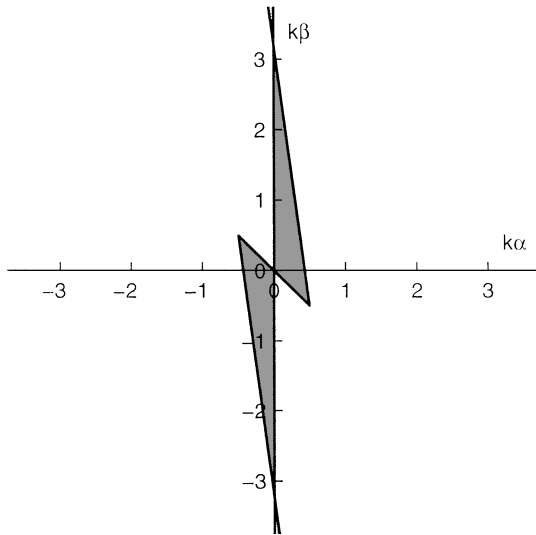


FIG. 3. Stability region for the linearly implicit AB4/AM2 method. The shaded portion indicates time stability of the method for choices of time step k and parameters α and β in (5).

Stability analysis of composite methods has been carried out before [2, 3]. For any combination of the real quantities $k\alpha$ and $k\beta$ we can determine whether growth in time is possible. From such data we can draw stability regions in the $k\alpha$ - $k\beta$ plane. Note that these pictures depend strongly on the assumption in (5) that the individual linearizations have imaginary spectra. Hence, different pictures must be generated for the analysis of convection-diffusion equations, for example.

We begin with the combination AB4/AM2, which combines high accuracy for the nonlinear term with an A -stable method for the linear term. The stability region is shown in Fig. 3. While the $k\beta$ -axis is included, as required by A -stability, we see that any nonzero α is likely to destabilize the method. We attribute this behavior to the fact that the imaginary axis is on the boundary of the classical stability region for AM2. The combination does indeed behave poorly in experiments with nonlinear wave equations. We use it to illustrate the importance of analyzing the interaction of the explicit and implicit methods as opposed to relying solely on their independent behaviors.

Figure 4 shows stability diagrams for the combinations AB4/AB4 (i.e., classical AB4), AB4/AM6, AB4/AM2*, and also the Chan & Kerkhoven (CK) scheme. Here AM2* denotes the usual AM2 scheme

$$y_{n+1} - y_n = \frac{k}{2}(y'_{n+1} + y'_n)$$

modified to

$$y_{n+1} - y_n = \frac{k}{2} \left(\frac{3}{2}y'_{n+1} + \frac{1}{2}y'_{n-1} \right).$$

This method is also second order accurate and A -stable when used by itself, but the imaginary axis is well in the interior of the stability region (i.e., AM2* is L -stable [12]). The stability of AB4/AM2* is greatly improved over that for AB4/AM2 (compare to Fig. 3).

We again note that for our purposes, α is nonzero and (at most wavenumbers) is much smaller than $\beta = \omega^m$. Hence we are interested in methods that have coverage far along and

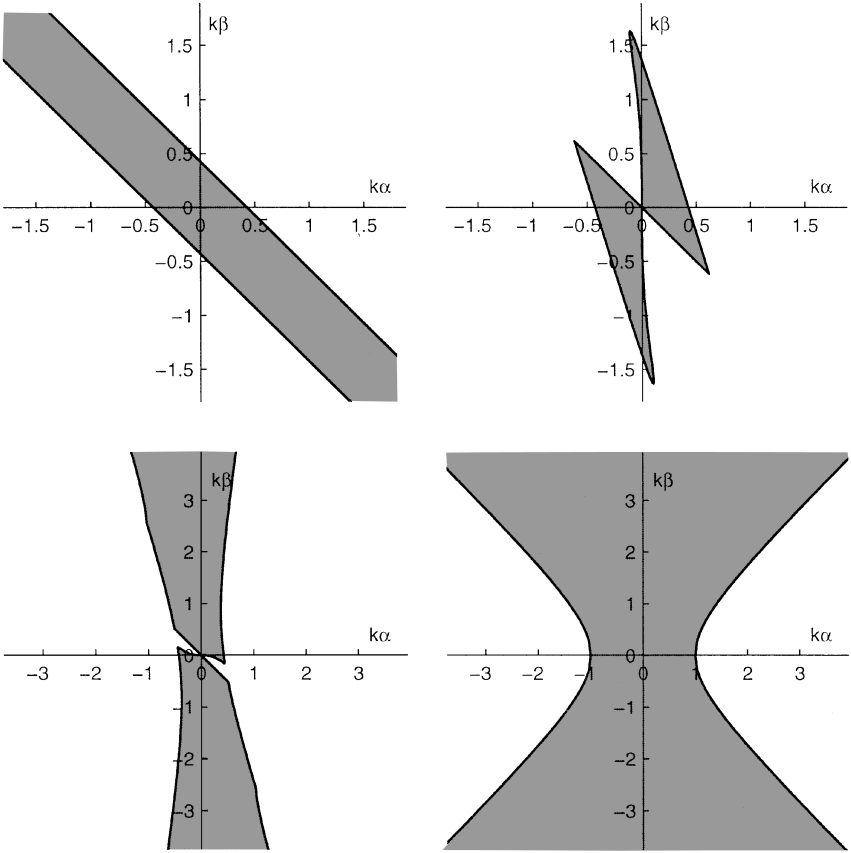


FIG. 4. Stability regions for linearly implicit AB/AM methods for (5). From upper left are AB4/AB4 (equivalent to classical AB4), AB4/AM6, AB4/AM2*, and the Chan and Kerkhoven method.

near the β -axis. Although CK effectively removes the stability limitation imposed by β , it suffers from low (second order) accuracy.

In the previous section, we proposed using different integrators for different ranges of the wavenumber. One idea would be to use ordinary AB4 for low values of $|\beta|$ and then switch to CK for high values. However, the small stability ordinate for AB4 forces the switch to CK at an undesirably small value of $k|\beta|$. We therefore improve further by using AB4/AM6 in a medium range. Figure 4 shows how this roughly triples the stability region along the β axis. (Although certain sectors of α and β are unstable for this method, this instability is so weak that it has no adverse effect, especially since the smallest $|\beta|$ -values are still handled by pure AB4.) The last modification is to substitute AB4/AM2* for CK, thus allowing a single explicit method for all β and improving the accuracy for the nonlinear part of the equation.

These considerations lead us to the present strategy:

Low $ \beta $	∴	Medium $ \beta $	∴	High $ \beta $
AB4/AB4	∴	AB4/AM6	∴	AB4/AM2*
	Cutoff		Cutoff	
	$ \beta = 0.43/k$		$ \beta = 1.36/k$	

We make a few observations.

- As $k \rightarrow 0$, our approach becomes a classical AB method.
- The cutoffs are derived from the usual stability ordinates of AB4 and AM6; they should perhaps be used conservatively due to nonzero α .
- The AB/AM stability regions are needed to justify the effectiveness of the linearly implicit combinations, but not for the implementation of the method.
- In some of the tests below, we have in a straightforward manner substituted AB7 for AB4.

5. NUMERICAL COMPARISONS

We restrict our comparisons to a few major numerical methods applied to the KdV and NLS equations. The methods we compare are:

LI: The present method of using linearly implicit Adams methods, with different methods selected for different wavenumber ranges.

CK: The method of Chan and Kerkhoven, as described in Section 2.

SS: The split-step Fourier method. In its simplest form (giving first order accuracy in time), one advances $u_t + A(u) + B(u) = 0$ by solving

$$u_t + 2A(u) = 0, \quad \text{from } t \text{ to } t + \frac{1}{2}k, \text{ followed by}$$

$$u_t + 2B(u) = 0, \quad \text{from } t + \frac{1}{2}k \text{ to } \left(t + \frac{1}{2}k\right) + \frac{1}{2}k = t + k.$$

The two time increments are each of the length $\frac{1}{2}k$; we denote this by $\{\frac{1}{2}, \frac{1}{2}\}$. One gets second-order accuracy in time by alternating A, B, A in the equations above while using the time increments $\{\frac{1}{4}, \frac{1}{2}, \frac{1}{4}\}$. Yoshida [18] showed a systematic way to find split-step methods of any even order. From an implementation standpoint, one simply chooses certain longer time increment sequences (while again alternating A, B, A, B, \dots). Table I lists the coefficients of methods of order 1, 2, 4, and 6.

The purpose of splitting is most often to alleviate stability limitations by permitting a linear subproblem to be solved analytically. When such linear problems are to be solved “back-to-back” in neighboring time steps, the adjoining substeps can be merged to improve

TABLE I
Coefficients of Split-Step Methods

Method	Time increment sequence (in general not unique)		
SS1	0.50000 00000 00000 00000	0.50000 00000 00000 00000	
SS2	0.25000 00000 00000 00000	0.50000 00000 00000 00000	0.25000 00000 00000 00000
SS4	0.33780 17979 89914 40851	0.67560 35959 79828 81702	-0.08780 17979 89914 40851
	-0.85120 71919 59657 63405	-0.08780 17979 89914 40851	0.67560 35959 79828 81702
	0.33780 17979 89914 40851		
SS6	0.19612 84026 19389 31595	0.39225 68052 38778 63191	0.25502 17059 59228 84938
	0.11778 66066 79679 06684	-0.23552 66927 04878 21832	-0.58883 99920 89435 50347
	0.03437 65841 26260 05298	0.65759 31603 41955 60944	0.03437 65841 26260 05298
	-0.58883 99920 89435 50347	-0.23552 66927 04878 21832	0.11778 66066 79679 06684
	0.25502 17059 59228 84938	0.39225 68052 38778 63191	0.19612 84026 19389 31595

efficiency. In solving NLS, split-step profits from the existence of a simple analytic solution for the nonlinear equation in physical space.

IF: The integrating factor method, as described in [13]. This has also been called “linearly exact” [7] and is related to exponential time stepping in electromagnetics [14]. To solve, say, NLS, we multiply (3) by $e^{i\omega^2 t}$ to obtain

$$\hat{v}_t = i e^{i\omega^2 t} \hat{N}(e^{-i\omega^2 t} \hat{v}), \quad (6)$$

where $\hat{v} = e^{i\omega^2 t} \hat{u}$. The stability restriction for (6) is relatively mild for any ODE method, but [7] points out that the error for this problem will be much larger than that of the original problem, because of the rapidly varying coefficient that has been introduced. In the present comparison we have used AB4 and AB7 (omitting AB5 and AB6 since they have zero stability ordinate).

We test the approaches discussed above on the KdV and NLS equations. In the SS methods the linear part was advanced analytically in Fourier space for both equations. Advancing the the nonlinear part of NLS is exact in physical space; for the KdV equation, the nonlinear part was advanced using a high-order Runge–Kutta integrator. Because this procedure is somewhat problematic for orders greater than four, SS6 was not implemented for the KdV case.

Figure 5 shows the analytical evolution from initial to final time of a two-soliton test case for KdV, and Figs. 6 and 7 display similarly our test case for the NLS equation. The test cases were discretized using 512 points in space, sufficient for roughly 10^{-12} computational accuracy for KdV and 10^{-8} for NLS. (Throughout the experiments we measure error in the L_2 norm relative to the initial condition.)

Figure 8 shows how the accuracy at the final time in KdV improves as smaller time steps are used. In order to make fair and robust comparisons, we measure computational effort in terms of the number of FFT evaluations, which measures well the total computational cost of these methods. In practice one wishes to time step as economically as possible while obtaining the full accuracy of the spatial discretization. We are therefore interested in the points in Fig. 8 at which the temporal errors have just reached the spatially imposed “floor,”

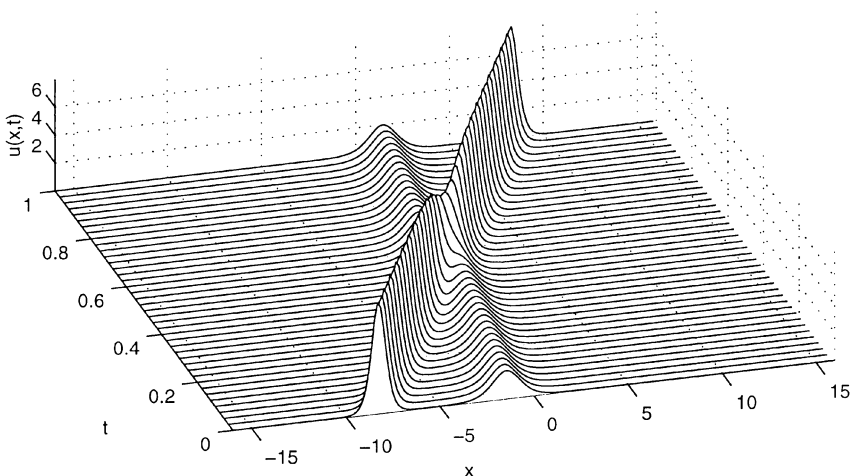


FIG. 5. Two-soliton test solution for KdV.

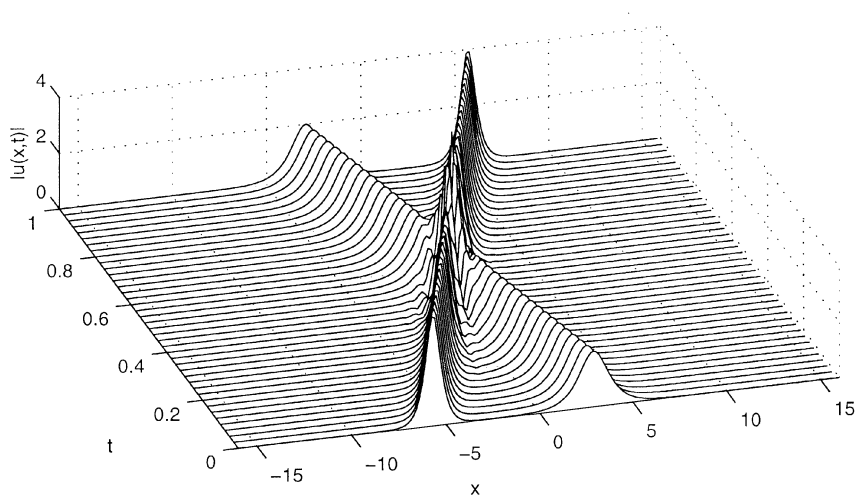


FIG. 6. Two-soliton solution for NLS, in magnitude.

as indicated by the boldface labels. (Convergence curves are extrapolated linearly where necessary.) A similar plot for NLS is shown in Fig. 9.

From these comparisons we note:

- For each time stepping method, the efficiency increases with the order of accuracy. The improvement is quite dramatic in going from order 2 to 4 but levels off somewhat in moving further to orders 6 and higher.
- Comparing methods of the same order, our LI method is more cost effective than the IF method, which in turn is superior to SS implementations.
- The performance gaps are larger for KdV than for NLS. This is presumably because

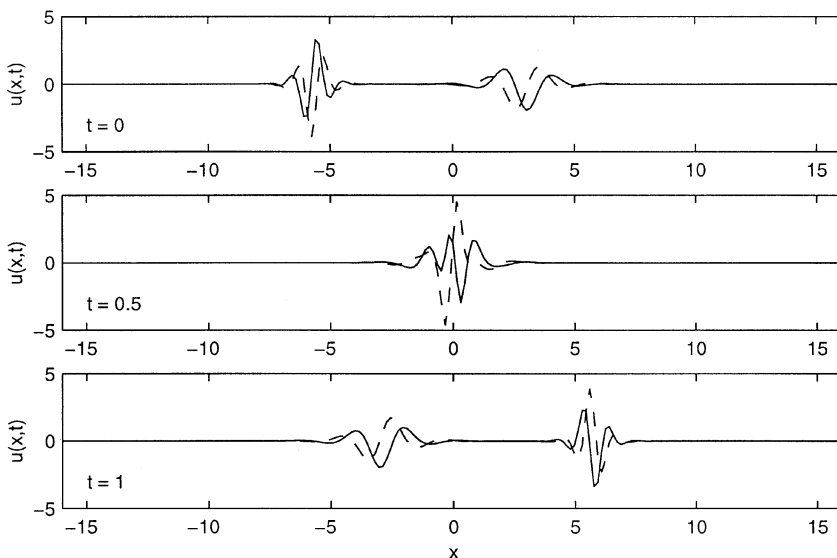


FIG. 7. Snapshots of real (solid) and imaginary (dashed) parts of the NLS solution of Fig. 6.

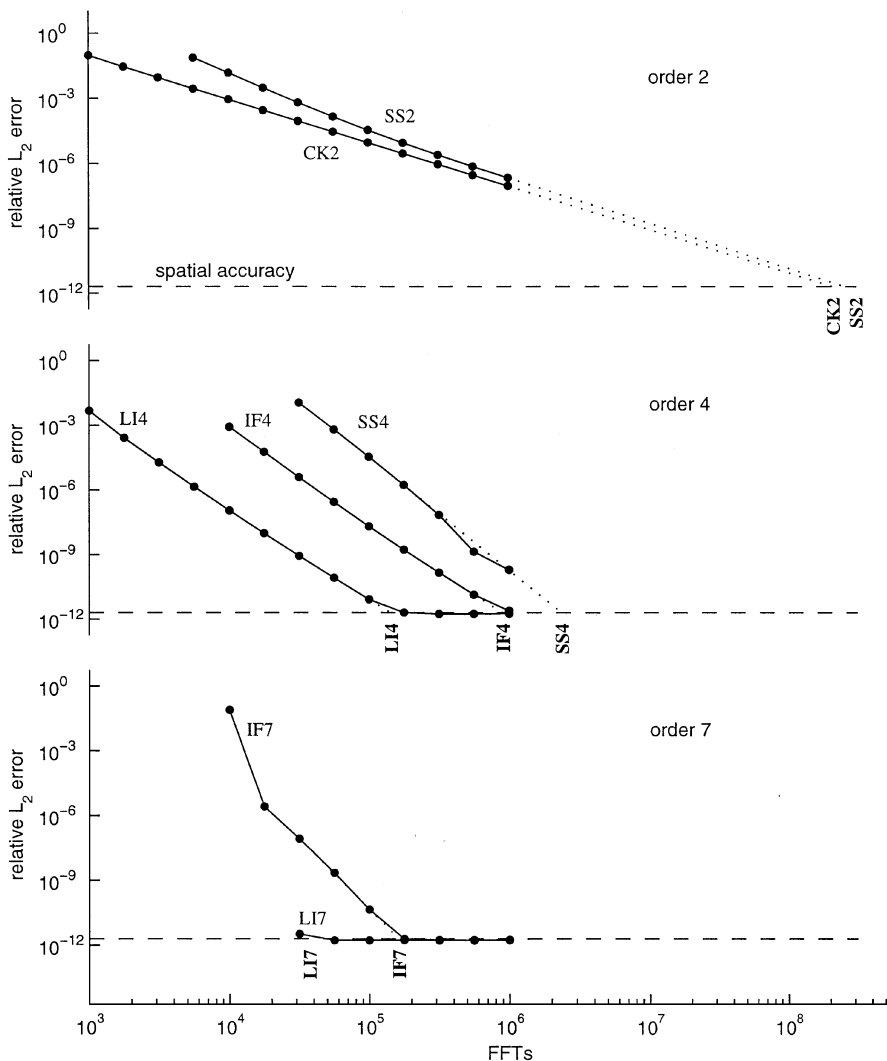


FIG. 8. Performance for KdV. For clarity, methods are grouped by order. Actual data are shown as filled circles; linear extrapolations are shown as dotted lines. The goal is to match spatial resolution (dashed lines) with as little cost (measured by counting FFTs) as possible. The point at which a method is estimated to achieve this matching is indicated by a boldface vertical label.

the u_{xxx} term in KdV is more stiff than is u_{xx} in NLS. (Also, split-step has an extra advantage in “pure” NLS, as pointed out above.)

All the numerical schemes that we have considered use a spectral representation in space. Classical (i.e., low-order) finite difference or finite element schemes are far more costly. For example, the second order explicit finite difference scheme for (KdV) by Zabusky and Kruskal [19],

$$u_j^{n+1} - u_j^{n-1} = 2\frac{k}{h}(u_{j-1}^n + u_j^n + u_{j+1}^n)(u_{j-1}^n - u_{j+1}^n) + \frac{k}{h^3}(u_{j-2}^n - 2u_{j-1}^n + 2u_{j+1}^n - u_{j+2}^n),$$

was used in pioneering the numerical computation of solitons. To reach our present

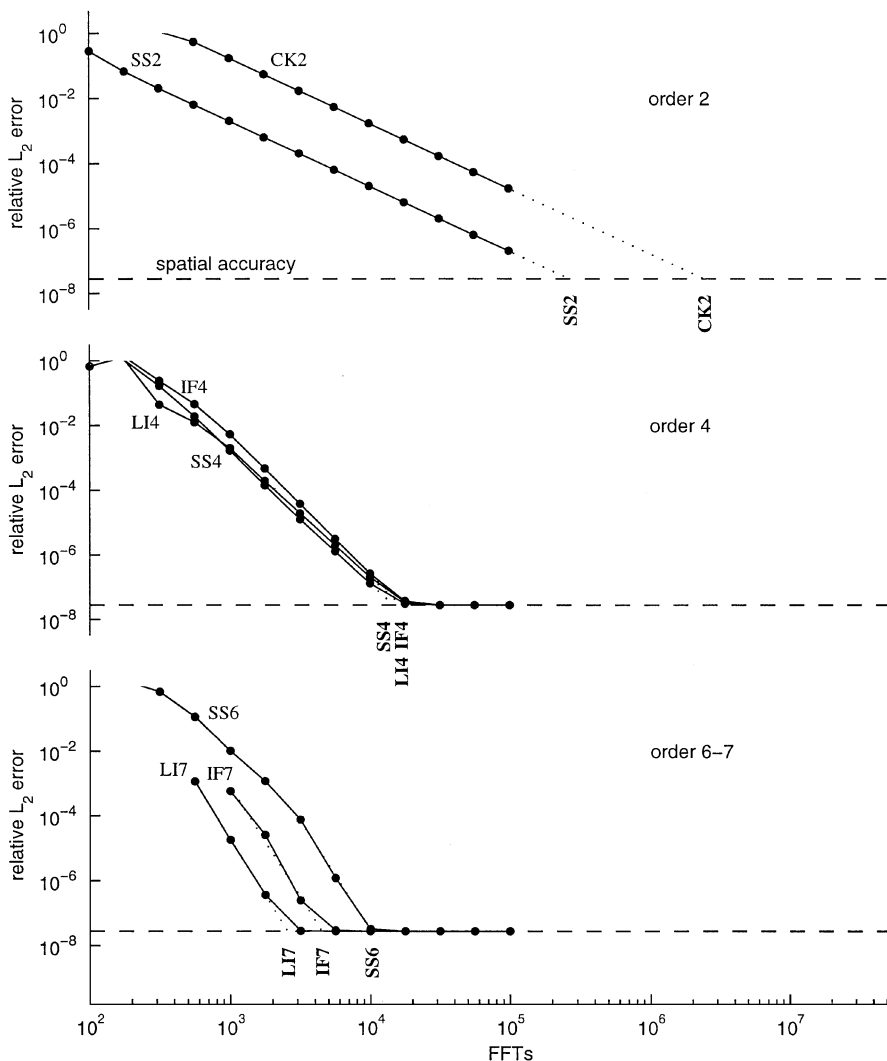


FIG. 9. Performance for NLS. (See Fig. 8 and the text for explanation.)

“accuracy floor” of 10^{-12} requires $h \approx 10^{-6}$. The asymptotic stability condition of $k/h^3 < 2/(3\sqrt{3})$ will then force $k \approx 10^{-18}$. The required computer time would become comparable to the estimated age of the universe.

6. CONCLUSIONS

In this study we have presented an easily implemented time stepping strategy for spatially spectral numerical solutions to a wide range of nonlinear wave equations. The method combines Adams–Bashforth and Adams–Moulton methods for the nonlinear and stiff linear parts, respectively, with the novel feature that different methods are used in different wavenumber ranges. The result combines high temporal accuracy with good stability properties. Numerical tests conducted on the KdV and NLS equations show that the new approach is computationally more effective than other currently available methods.

REFERENCES

1. U. M. Ascher, S. J. Ruuth, and R. J. Spiteri, Implicit–explicit Runge–Kutta methods for time-dependent partial differential equations, *Appl. Num. Math.* **25**, 151 (1997).
2. U. M. Ascher, S. J. Ruuth, and B. T. R. Wetton, Implicit–explicit methods for time-dependent partial differential equations, *SIAM J. Numer. Anal.* **32**, 797 (1995).
3. M. P. Calvo, J. de Frutos, and J. Novo, *Linearly Implicit Runge–Kutta Methods for Advection–Reaction–Diffusion Equations*, Technical Report 1999/3 (Universidad de Valladolid, Valladolid, Spain, 1999).
4. C. Canuto, M. Y. Hussaini, A. Quarteroni, and T. A. Zang, *Spectral Methods in Fluid Dynamics* (Springer-Verlag, Berlin, 1988).
5. T. F. Chan and T. Kerkhoven, Fourier methods with extended stability intervals for the Korteweg–de Vries equation, *SIAM J. Numer. Anal.* **22**, 441 (1985).
6. B. Fornberg, *A Practical Guide to Pseudospectral Methods* (Cambridge University Press, Cambridge, UK, 1996).
7. B. García-Archilla, Some practical experience with the time integration of dissipative equations, *J. Comput. Phys.* **122**, 25 (1995).
8. M. Ghrist, *High-order Finite Difference Schemes for Wave Equations*, Ph.D. thesis (University of Colorado, Boulder, CO, in preparation.)
9. M. Ghrist, T. A. Driscoll, and B. Fornberg, Staggered time stepping methods for wave equations, submitted.
10. B. Gustafsson, H.-O. Kreiss, and J. Olinger, *Time Dependent Problems and Difference Methods* (Wiley, New York, 1995).
11. E. Hairer, S. P. Nørsett, and G. Wanner, *Solving Ordinary Differential Equations I: Nonstiff Problems*, 2nd ed. (Springer-Verlag, Berlin, 1993).
12. E. Hairer and G. Wanner, *Solving Ordinary Differential Equations II: Stiff and Differential–Algebraic Problems*, 2nd ed. (Springer-Verlag, Berlin, 1996).
13. P. A. Milewski and E. G. Tabak, A pseudo-spectral procedure for the solution of nonlinear wave equations with examples from free-surface flows, *SIAM J. Sci. Comput.*, in press.
14. A. Taflove, *Computational Electrodynamics: The Finite-Difference Time-Domain Method* (Artech House, Boston, 1995).
15. T. R. Taha and M. J. Ablowitz, Analytical and numerical aspects of certain nonlinear evolution equations. I. Analytical, *J. Comput. Phys.* **55**, 192 (1984).
16. T. R. Taha and M. J. Ablowitz, Analytical and numerical aspects of certain nonlinear evolution equations. II. Numerical, nonlinear Schrödinger equation, *J. Comput. Phys.* **55**, 203 (1984).
17. T. R. Taha and M. J. Ablowitz, Analytical and numerical aspects of certain nonlinear evolution equations. III. Numerical, Korteweg–de Vries equation, *J. Comput. Phys.* **55**, 231 (1984).
18. H. Yoshida, Construction of higher order symplectic integrators, *Phys. Lett. A* **150**, 262 (1990).
19. N. J. Zabusky and M. D. Kruskal, Interaction of “solitons” in a collisionless plasma and the recurrence of initial states, *Phys. Rev. Lett.* **15**, 240 (1965).